Received: April 16, 2024. Revised: May 14, 2024.

INASS

International Journal of
Intelligent Engineering & Systems

http://www.inass.org/

Design of a Robust PID-PSS & FACTS Using Craziness Particle Swarm Optimization in Sulselrabar System

Makmur Saini[1] Muhammad Ruswandi Djalal[1]* A.M. Shiddiq Yunus[1]

[1]*Department of Mechanical Engineering, State Polytechnic of Ujung Pandang, Makassar 90245, Indonesia*
* Corresponding author's Email: wandi@poliupg.ac.id

Abstract: This research delves into enhancing the efficiency and stability of the Sulselrabar system by employing Proportional Integral Derivative (PID)-Power System Stabilizer (PSS) and Flexible AC Transmission System (FACTS) controls. The proposed control approach integrates PID-PSS1A for PSS and Static Var Compensator (SVC) for the FACTS device. Achieving optimal performance necessitates a coordinated strategy, thus this study incorporates optimization techniques for PID-PSS and SVC. It utilizes the artificial intelligence method Craziness Particle Swarm Optimization (CRPSO) for optimization, with conventional Particle Swarm Optimization (PSO) employed for comparison purposes. Analysis of SVC indicates that the recommended placement and capacity for bus 31 are determined as 40 MVar, while the CRPSO method suggests an optimal rating of 80 MVar. The implementation of CRPSO-based PID-PSS-SVC presents minimum power losses, namely active power is reduced to 8.7% and reactive power is reduced to 3.8%, while stability increases through damping system analysis by 25.13%.

Keywords: PID, PSS, FACTS, Sulselrabar, CRPSO.

1. Introduction

Disturbances frequently occur in electric power systems, manifesting as transients or load changes [1]. Such disturbances instigate instability within the system, which can manifest as frequency instability, rotor angle instability, or voltage instability [2, 3]. Typically, instability is affected by initial conditions and the magnitude of the disturbance. The disturbances directly affect variations in electrical power, subsequently impacting mechanical power. One contributing factor to instability is the mismatch in response times between rapid electrical power responses and slower mechanical power responses. This discrepancy often leads to oscillations within the system.

Electric power systems necessitate both voltage stability and optimal power flow. Changes in load conditions can lead to voltage instability, resulting in under-voltage and over-voltage scenarios. To maintain this stability, reactive power compensation becomes crucial [4]. During instances of under-voltage and over-voltage, power modulation is achieved using a type of Flexible AC Transmission System (FACTS) equipment, specifically the Static Var Compensator (SVC) [5]. The SVC comprises thyristor-controlled reactor (TCR) and capacitor components. Meanwhile, disturbances in the form of electrical power oscillations are typically addressed with additional equipment such as the Power System Stabilizer (PSS). The role of the PSS is to enhance stability by providing damping to generator oscillations. PSS damping involves generating an electrical torque component that is in phase with changes in speed.

Several other types of FACTS equipment exist, including the Static Synchronous Compensator (STATCOM), Static Synchronous Series Compensator (SSSC), Unified Power Flow Controller (UPFC), and Thyristor Controlled Series Compensator (TCSC) [6]. These controllers play a crucial role in enhancing the controllability and efficiency of power systems. FACTS controllers can significantly influence the steady-state performance of a power system, with their impact depending on factors such as capacity, type, and placement [7].

However, incorporating these factors into the Optimal Power Flow (OPF) problem poses a highly intricate optimization challenge. As a result, heuristic optimization methods are frequently utilized to effectively address this issue [8].

The literature has proposed several approaches to solve the OPF problem in the presence of FACTS devices. These approaches often utilize metaheuristic methods such as Particle Swarm Optimization (PSO) [9], Opposition Krill Herd Algorithm (OKHA) [10], Symbiotic Organisms Search (SOS) [11], Success History-based Adaptive Differential Evolution (SHADE) [12], Efficient Parallel Genetic Algorithm (EPGA) [13], Grasshopper Optimization Algorithm (GOA) dan Integrated Ant Lion Optimizer (IALO) [14]. Moreover, conventional techniques like Sequential Quadratic Programming [15] and the Newton method have also been applied [16]. These various methods provide a spectrum of optimization strategies to address the intricacies of the OPF problem when FACTS devices are involved.

Many comparative studies have examined the effectiveness of metaheuristic algorithms in tackling engineering challenges, as demonstrated in [17]. Literature reviews indicate that the use of metaheuristic algorithms for solving engineering problems, particularly the OPF problem, is becoming increasingly common. These algorithms frequently produce optimal computational results, especially in power system applications. Previous research [18] investigated the deployment of FACTS, particularly SVC, in the South Sulawesi system for optimal power flow using PSO. The optimization results indicate that improving power flow enhances the performance of the South Sulawesi system. However, the PSO method utilized in this study exhibits limitations. While conventional PSO methods provide optimal solutions to optimization problems, their performance encounters challenges, particularly with the particle velocity function. Additionally, stability problems, especially during N-1 contingency conditions and variations in load changes in this study, have not been studied in detail. In this study, we introduce an approach that utilizes the Craziness Particle Swarm Optimization (CRPSO) metaheuristic method to tackle the placement and rating problem of SVC and PSS.

Based on the literature studies above, many algorithms demonstrate issues such as premature convergence, stagnation, and repeatedly revisiting the same solution. To address this issue, the PSO algorithm has been modified in this paper. In the context of a flock of birds or a school of fish, sudden changes in direction are common. This behavior is elucidated by introducing a ‘craziness’ factor, which is incorporated into the technique through the craziness variable. The craziness operator is introduced in the proposed technique to guarantee that each particle maintains a predetermined probability of exhibiting craziness, thereby preserving particle diversity. The algorithm’s performance is evaluated through comparison with the conventional PSO algorithm.

The CRPSO method represents an advancement over the conventional PSO method [19], demonstrating promising results across various applications in power system optimization. Research [20] utilizes CRPSO to optimize and determine the appropriate Proportional Integral Derivative (PID) parameters for a Permanent Magnet Synchronous Motor (PMSM). Based on the simulation results, CRPSO demonstrates superior performance compared to PSO, exhibiting minimal overshoot response across various speed variations. Furthermore, CRPSO leads to an increase in the starting torque of the PMSM. In paper [21], an enhanced version of PSO known as CRPSO is explored as an efficient optimization tool for designing Infinite Impulse Response (IIR) digital filters. Beyond simply enhancing control over the cognitive and social components of traditional PSO, CRPSO achieves superior performance by incorporating inertia parameters into the PSO speed equation.

This research conducts a case study focusing on the power system of South, Southeast, and West Sulawesi (Sulselrabar). We employ the CRPSO optimization technique to address the OPF problem while considering the devices within the power system network that constitute FACTS. The following summarizes the contributions of this paper:

- Implementation of the CRPSO algorithm for solving the OPF and Stability problem in the Sulselrabar power system.
- Addressing undervoltage and overvoltage issues, as well as power losses, through OPF using SVC deployment.
- Enhanced stability is achieved by optimizing the performance of a CRPSO-based PID-PSS system to maximize damping in N-1 contingency conditions.

The paper is structured into distinct sections. Section II provides an overview of the Sulselrabar linear model, while Section III delineates the research methodology. Section IV delves into the results obtained from the applied method, and Section V offers the research conclusions.

2. System model

2.1 SVC modeling

A device capable of injecting or absorbing reactive power is referred to as a shunt compensator, commonly known as SVC. When connected in parallel, these devices have the capability to modify the flow of reactive power at their connection point [22]. In essence, an SVC operates as a variable inductor or capacitor. Thyristor-switched reactors and thyristor-controlled capacitors are shunt-connected to the power system. The static SVC model is depicted in Fig. 1. Eq. (1) is a correlation depicting the reactive power either injected into or absorbed from a bus by an SVC:

$$Q_{svc} = V^2 B_{svc} \tag{1}$$

B_{svc} stands for susceptance, and V represents the voltage of the bus.

Optimal SVC Placement

The optimal positioning of the SVC is determined by analyzing the power-voltage (PV) curve. This curve is constructed using advanced power flow techniques, particularly the OPF method.

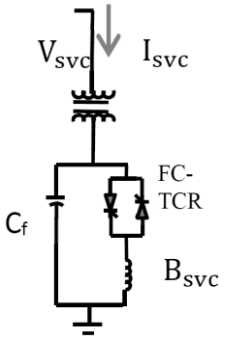

Figure. 1 SVC Static Models

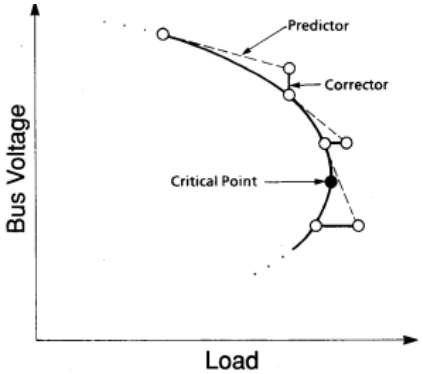

Figure. 2 The predictor and corrector scheme employed in OPF [23]

Conventional power flow methods face difficulties at points of bifurcation or maximum load capability because of singularities in the Jacobian matrix. Consequently, OPF was developed to examine power flow across all load locations with minor adjustments to the power flow equations. OPF utilizes predictor and corrector schemes to ascertain power flow solutions at all load points, as depicted in Fig. 2.

Additional information regarding OPF can be found in [23]. The OPF method addresses concerns associated with singularities in the Jacobian matrix, enabling the generation of PV curves for any system across different load points. PV curves are generated for all load buses, and buses exhibiting notable voltage fluctuations in response to load changes are recognized as weak buses, indicating their potential suitability for SVC installation. OPF is a resilient technique and is readily available through numerous commercial software packages.

2.2 Excitation-PID-PSS system modeling

The exciter type employed is a fast exciter, as depicted in Fig. 3. This particular type of exciter effectively mitigates negative damping, which could hinder torque attenuation. Eq. (2) [24] provides the formal expression for the fast exciter.

$$E_{fd} = K_A\left(V_t - V_{ref}\right)/(1 - T_A s) \tag{2}$$

K_A represents the gain, and T_A represents the time constant. To accommodate equipment constraints, the output of this exciter must be confined within the range of V_{Rmin} to V_{Rmax}, where V_{Rmin} is the minimum value and V_{Rmax} is the maximum voltage value. The block diagram for the fast exciter is illustrated in Fig. 3.

Eq. (3) describes the output of the PSS. K_{PSS} denotes the PSS gain, T_w represents the washout filter, and T_A, T_B, T_C, and T_D represent the lead-lag gains.

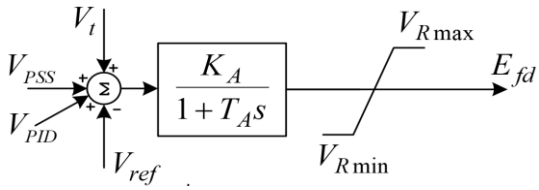

Figure. 3 Exciter Model

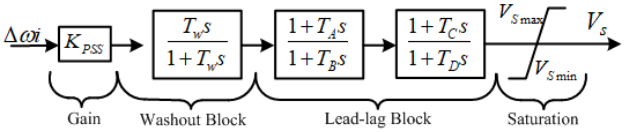

Figure. 4 Block Diagram of PSS1A

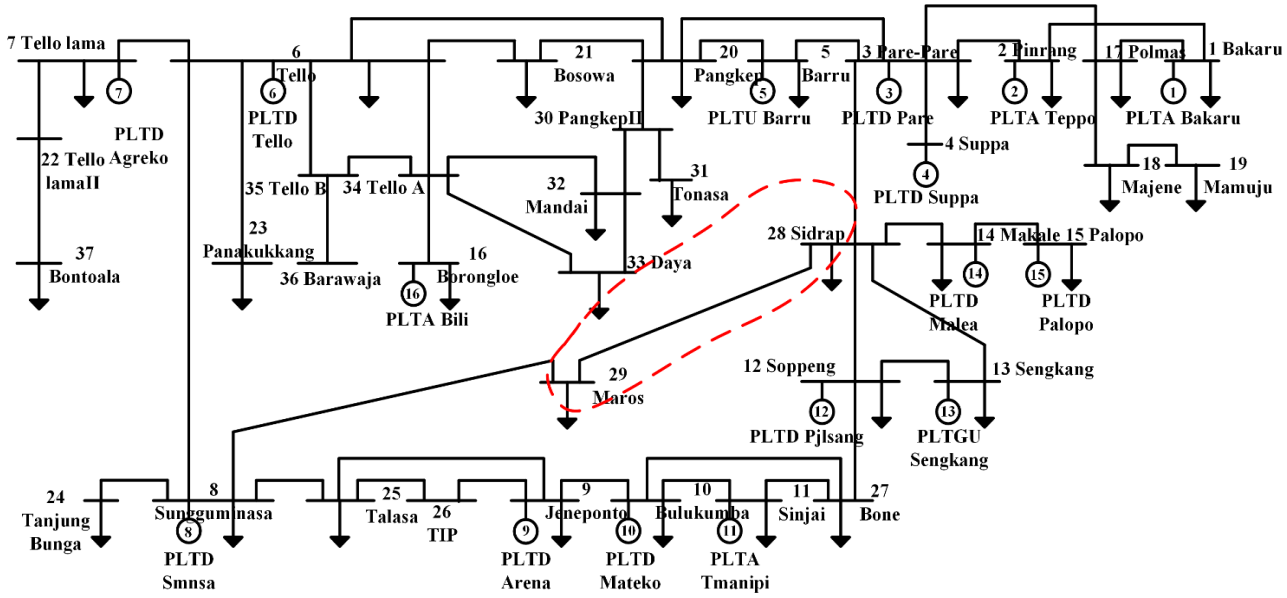

Figure. 5 Test System

Additionally, V_{Rmax} and V_{Rmin} are the limiters utilized. The PSS operates by supplying an additional signal to the generator excitation. For a graphical representation of the conventional single-input PSS1A modeling, please refer to Fig. 4.

$$V_s = K_{pss}\frac{T_w s}{1+T_w s}\left[\frac{(1+sT_A)}{(1+sT_B)}\frac{(1+sT_C)}{(1+sT_D)}\right]\omega \qquad (3)$$

To handle these input signals, transducer and washout circuits are employed. The transducer is tasked with converting the input signal into a voltage signal, while the washout circuit ensures steady conditions at the stabilizer's output.

2.3 Test system

The South, Southeast, and West Sulawesi regions (Sulselrabar) are interconnected via the Sulselrabar system, comprising 46 transmission lines connecting primary load centers and 16 generators. This system operates with 37 buses at 150 kV. To facilitate analysis, bus numbers are assigned. The bus numbers for the Sulselrabar electrical system are depicted in Fig. 5. Additionally, Fig. 5 illustrates the case study utilized in this research, which analyzes the performance of the South Sulawesi system in response to the N-1 contingency on the Maros-Sidrap Central route.

3. Craziness particle swarm optimization

PSO is an optimization technique based on populations. It begins by dispersing a group of particles throughout a problem space, forming what is termed as a swarm [19]. Each particle within the swarm holds data regarding its own position and the potential value associated with that position. These particles interact with each other, exchanging information about the best positions discovered thus far. This shared knowledge assists each particle in adjusting its movement towards more favorable positions. The movement is guided by a velocity function. Each particle in the swarm calculates its position during flight by considering both its own best experience (P_{best}) and the collective best experience (G_{best}). The PSO concept can be mathematically expressed using Eqs. (4) and (5).
Particle velocity updates:

$$v_i^{k+1} = v_i + c_1 r_1\left(Pbest_i - x_i^{k}\right) + c_2 r_2\left(Gbest_i - x_i^{k}\right) \qquad (4)$$

Update particle position:

$$x_i^{k+1} = x_i + v_i^{k+1} \qquad (5)$$

x^k represents the current search point, x^{k+1} denotes the modified search position, v^k indicates the current speed, v^{k+1} signifies the modified speed, V_{pbest} represents the speed based on P_{Best}, V_{gBest} denotes the speed based on G_{best}, n stands for the number of particles in a group, m represents the number of members in the particle, $p_{best\text{-}i}$ signifies P_{best} from the current iteration, $g_{best\text{-}i}$ represents G_{best} from the group, w stands for the weight, c_i is the weight coefficient for the following terms:

- c_1 and c_2 are two positive constants,
- r_1 and r_2 are random numbers ranging from 0-1.

Table 1. CRPSO Parameters

Particles (P_{craz})	30
Iteration	50
Variables	3
Social Constant, C2	2
Cognitive Constant, C1	2
Weight Min & Max CRPSO	0.9 & 0.4

Traditional PSO is prone to premature convergence, often leading to the solution being trapped in a local optimum. In contrast, CRPSO introduces modifications to the velocity update function, enabling particles to occasionally exceed velocity constraints in certain iterations. These iterations are determined by a probability known as a "crazy particle." The value of the crazy particle is influenced by weight adjustments that occur in each iteration, as depicted in Eqs. (6) and (7) below.
Particle updates weight [25]:

$$w^k = (w_{max} - w_{min}) \times \frac{iter_{max} - iter^k}{iter_{max}} + w_{min} \quad (6)$$

$$P_{craz} = w_{min} - exp\left(-\frac{w^k}{w_{max}}\right) \quad (7)$$

The adjustments made to the update velocity based on the P_{craz} value, which represents the probability of a particle being considered as a 'crazy particle,' are depicted in Eq. (8) as follows.

$$v_i^k = \begin{cases} rand\ (0, v_{max}) & If\ P_{craz} \leq rand\ (0,1) \\ v_i^k & Others \end{cases} \quad (8)$$

The CRPSO parameters used in this study are summarized in Table 1.

3.1 SVC objective function

Optimizing a single objective function, the primary aim of solving the OPF problem is to enhance the steady operation of the power system over time. This task involves selecting suitable operational parameters while taking into account various technical and economic constraints imposed by both the equipment and the electrical grid. Mathematically, this is depicted as a nonlinear optimization challenge, for example:

Minimize f(x)
Subject to: g(x) = 0
h(x) ≤ 0

In this context, the variable *'x'* represents a collection of control and state parameters. The function *'f(x)'* represents the objective function, while *'h(x)'* and *'g(x)'* denote sets of inequality and equality constraints, respectively. The state variables comprise voltage and angle measurements at load buses, while the control variables encompass the active and reactive power outputs of generators, bus voltages, and transformer tap settings [26].

The objective function to minimize in this case is the active power loss within the transmission network, represented as follows Eq. (9) [27]:

$$\sum_k^N = 1 g_k \left[V_i^2 + V_j^2 - 2V_iV_j cos\theta_{ij}\right] \quad (9)$$

g_k represents the conductance of the connection between nodes *i* and *j*, where V_i and V_j denote the electrical potentials at these nodes, and B_{ij} indicates the angular disparity. *N* signifies the total number of transmission lines.

3.2 PID-PSS objective function

The resultant mathematical model is transformed into a state-space depiction, as demonstrated in Eqs. (10) and (11).

$$\Delta\dot{x} = A\Delta x + B\Delta u \quad (10)$$

$$\Delta y = C\Delta x + D\Delta u \quad (11)$$

Stability assessment of the system can be established by examining Matrix A through Eq. (12).

$$\det(sI\text{-}A)=0 \quad (12)$$

The analysis involves employing the identity matrix (denoted as *I*) and the eigenvalues (represented as *s*) of matrix *A*, which is of size *n x n*. Eq. (13) can be employed to determine the total count of eigenvalue systems.

$$\lambda_i = \sigma_i + j\omega_i \quad (13)$$

$$f = \frac{\omega}{2\pi} \quad (14)$$

Eq. (14) defines the oscillation frequency, where λ_i represents the eigenvalue, σ_i indicates the real component of the eigenvalue, and ω_i denotes the imaginary component of the eigenvalue. The damping aspect of the system is portrayed in the real eigenvalue segment, whereas the oscillatory aspect is depicted in the imaginary eigenvalue segment. Eq. (15) offers the computation for the damping value. The Comprehensive Damping Index (CDI), depicted

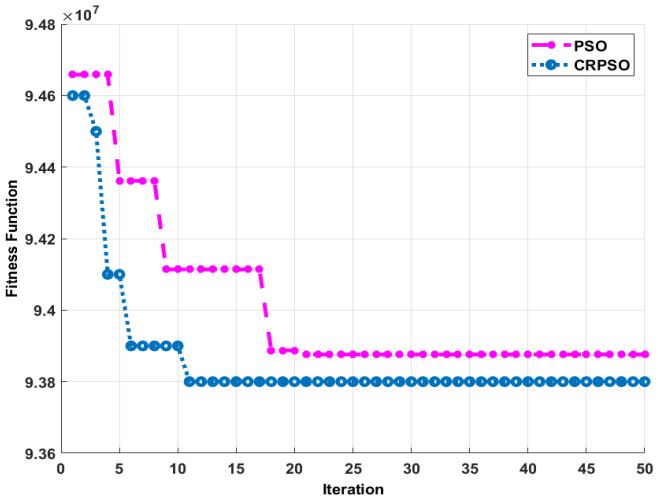

Figure. 6 Convergence Graph

in Eq. (16), provides an evaluation of the system's overall damping.

$$\zeta_i = \frac{-\sigma_i}{\sqrt{\sigma_i^2+\omega_i^2}} \quad (15)$$

$$CDI = \sum_{i=1}^{n}(1-\zeta_i) \quad (16)$$

The system's damping ratio is denoted as ζ_i, while the sum of the eigenvalues is represented by n. The primary objective of CRPSO is to maximize the minimum damping (ζ_{min}). The parameter limits for PID-PSS optimized using CRPSO are as follows: $K_{pss(min)} \leq K_{pss} \leq K_{pss(max)}$; $T_{1(min)} \leq T_1 \leq T_{1(max)}$; $T_{2(min)} \leq T_2 \leq T_{2(max)}$; $T_{3(min)} \leq T_3 \leq T_{3(max)}$; and $T_{4(min)} \leq T_4 \leq T_{4(max)}$, *and* $K_{P(min)} \leq K_P \leq K_{P(max)}$; $K_{I(min)} \leq K_I \leq K_{I(max)}$; *and* $K_{D(min)} \leq K_D \leq K_{D(max)}$.

3.3 CRPSO performance

Fig. 6 depicts the optimization process of SVC using PSO and CRPSO, showcasing a convergence plot. The computational analysis was conducted over 50 iterations to ascertain the optimal placement and adjustment for SVC. The PSO-driven optimization method reaches the optimal solution by the 21st iteration, with a minimum fitness function value of 9.39e+07. In contrast, CRPSO demonstrates faster convergence, achieving a fitness function value of 9.38E+07 by the 11th iteration.

4. Results and Discussion

4.1 SVC optimization

Initially, the investigation focused on analyzing the power flow of the Sulselrabar system prior to the installation of the SVC. Fig. 5 demonstrates that the N-1 contingency channel on the Maros and Sidrap middle lines forms the foundation for the case study utilized to identify the optimal SVC implementation. Table 2 presents a comparison of the results before and after optimization using PSO and CRPSO. The optimization results emphasize the optimal voltage profile, phase angle, and SVC placement. Before adjusting the SVC placement, power flow studies indicated that several bus voltage profiles were in marginal or critical conditions. As per the system operating regulations, a variation of ±5% in the minimum bus voltage is allowed. The following buses are experiencing marginal and critical conditions, as indicated in the currently available table:

- Marginal conditions: Bus 19, 23, 30, and 37.
- Critical conditions: Bus 31.

Bus 31 was found to be the best position for the SVC's placement and tuning after an artificial intelligence optimization analysis based on either PSO or CRPSO was conducted on the Sulselrabar system. When the SVC parameter was optimized with the PSO approach, the outcome was 40 MVar. However, when optimized with the CRPSO method, the results varied, yielding both 40 MVar and 80 MVar options. The voltage profile of the Sulselrabar bus system is shown in Fig. 7 both prior to and following SVC installation. The bus voltage profile has improved as a result of the SVC installation, moving from marginal and critical situations to normal operating conditions.

Enhancing and optimizing power flow within the transmission system is another benefit of the reactive power injection from the SVC. Reductions in active and reactive power losses are the outcomes of this improved power flow. Reducing power losses through increased optimal power flow in the system eventually improves the entire power transmission network's dependability and efficiency. The comparison of active and reactive power loss patterns using the PSO and CRPSO methods before and after SVC installation is shown in Figs. 8 and 9. There were 26.46695167 MW of active power losses before the SVC installation. It dropped to 24.52881713 MW after the SVC was installed and optimized using PSO; utilizing the suggested CRPSO approach, it was 24.16326638 MW. Prior to the SVC installation, reactive power losses were 60.49049752 MVar.

They decreased to 59.29182879 MVar after the SVC was installed and optimized using PSO. Using the suggested CRPSO approach, they decreased to 58.14185295 MVar. This decrease in power losses demonstrates how the SVC improves power flow, raises voltage, and lowers system losses.

Table 2. Voltage Profile

Voltage before Optimization					Voltage after Optimization With PSO				Voltage after Optimization With CRPSO			
Bus No	Voltage Mag	Angle Degree	Injected MVar	SVC MVar	Voltage Mag	Angle Degree	Injected MVar	SVC MVar	Voltage Mag	Angle Degree	Injected MVar	SVC MVar
1	1	0	0	0	1	0	0	0	1	0	0	0
2	1	-4.121	0	0	1	-4.09	0	0	1	-4.182	0	0
3	1	-5.485	0	0	1	-5.441	0	0	1	-5.574	0	0
4	1	-4.403	0	0	1	-4.358	0	0	1	-4.491	0	0
5	1	-11.578	0	0	1	-11.508	0	0	1	-11.705	0	0
6	1	-26.241	0	0	1	-25.985	0	0	1	-26.098	0	0
7	1	-26.641	0	0	1	-26.385	0	0	1	-26.498	0	0
8	1	-26.358	0	0	1	26.107	0	0	1	-26.221	0	0
9	1	-20.899	0	0	1	-20.69	0	0	1	-20.807	0	0
10	1	-16.238	0	0	1	-16.066	0	0	1	-16.187	0	0
11	1	-14.237	0	0	1	-14.082	0	0	1	-14.205	0	0
12	1	-2.518	0	0	1	-2.428	0	0	1	-2.556	0	0
13	1	3.27	0	0	1	3.347	0	0	1	3.217	0	0
14	1	-10.068	0	0	1	-10.005	0	0	1	-10.136	0	0
15	1	-12.076	0	0	1	-12.014	0	0	1	-12.145	0	0
16	1	-26.363	0	0	1	-26.147	0	0	1	-26.296	0	0
17	0.992	-3.223	0	0	0.992	-3.204	0	0	0.992	-3.26	0	0
18	0.974	-5.369	0	0	0.974	-5.35	0	0	0.974	-5.406	0	0
19	0.964	-6.538	0	0	0.964	-6.52	0	0	0.964	-6.576	0	0
20	0.975	-20.077	0	0	0.988	-20.077	0	0	1	-20.42	0	0
21	0.98	-22.788	0	0	0.988	-22.663	0	0	0.995	-22.896	0	0
22	0.987	-26.625	0	0	0.987	-26.369	0	0	0.987	-26.482	0	0
23	0.96	-28.482	10	0	0.96	-28.226	10	0	0.96	-28.339	10	0
24	0.993	-27.094	0	0	0.993	-26.843	0	0	0.993	-26.956	0	0
25	0.993	-25.113	0	0	0.993	-24.875	0	0	0.993	-24.99	0	0
26	0.993	-23.723	0	0	0.993	-23.494	0	0	0.993	-23.61	0	0
27	0.988	-10.485	0	0	0.988	-10.355	0	0	0.988	-10.479	0	0
28	0.996	-3.36	0	0	0.996	-3.297	0	0	0.996	-3.428	0	0
29	0.997	-26.778	0	0	0.997	-26.527	0	0	0.997	-26.641	0	0
30	0.954	-19.76	0	0	0.968	-20.667	0	0	0.98	-21.832	0	0
31	0.927	-20.791	10	0	0.967	-22.444	10	80	1.002	-24.29	10	40
32	0.98	-26.551	0	0	0.981	-26.403	0	0	0.982	-26.615	0	0
33	0.984	-26.614	0	0	0.985	-26.422	0	0	0.985	-26.593	0	0
34	0.993	-26.141	0	0	0.993	-25.919	0	0	0.993	-26.062	0	0
35	0.997	-26.191	0	0	0.997	-25.952	0	0	0.996	-26.08	0	0
36	0.997	-26.192	0	0	0.997	-25.952	0	0	0.996	-26.08	0	0
37	0.975	-27.924	0	0	0.975	-27.669	0	0	0.975	-27.781	0	0

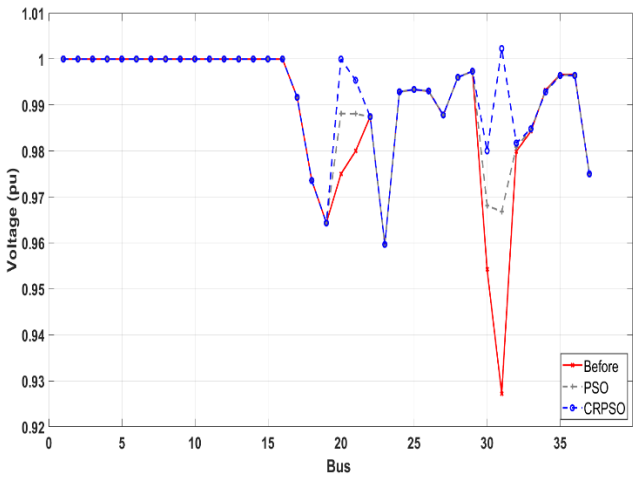

Figure. 7 Bus Voltage before and after adding SVC

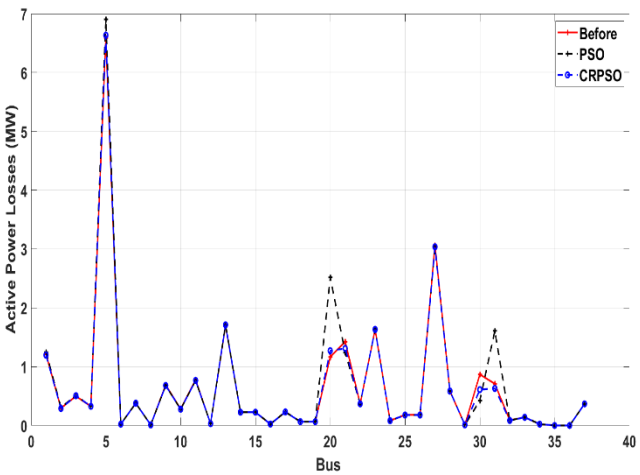

Figure. 8 Active Power Losses Profile

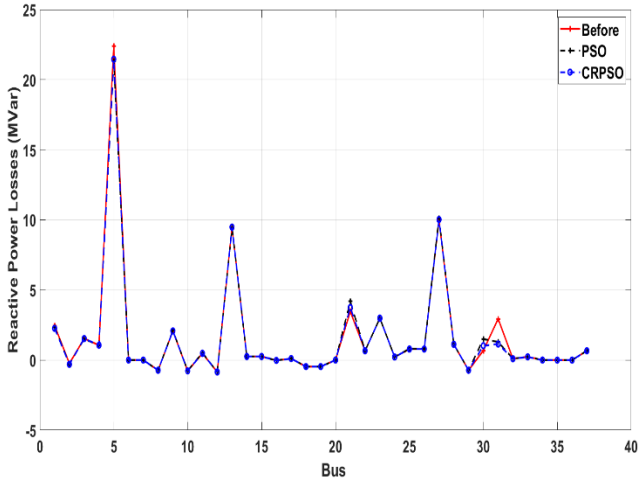

Figure. 9 Reactive Power Losses Profile

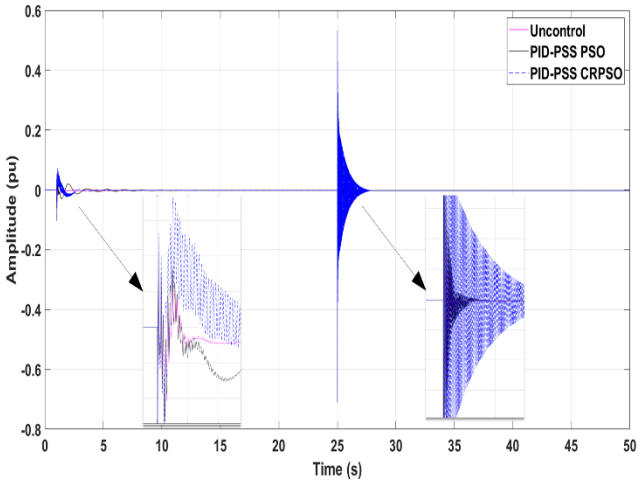

Figure. 10 Excitation output voltage (E_{fd}) of Bakaru

4.2 PID-PSS optimization

The optimization of PID-PSS was conducted through a case study involving variations in load changes on the Bakaru swing generator, as illustrated in Table 3. The variations in load changes occurred as follows: in the first second of operation, the generator experienced an additional load change of 0.1 pu; then, in the second, there was a decrease of 25 in additional load of 0.1 pu. Evaluation of the installation of PID-PSS on the South Sulawesi system was performed using the Time Domain Simulation (TDS) analysis method, specifically analyzing PSS field voltage response (E_{fd}), speed response ($\Delta\omega$), and rotor angle response (δ). Additionally, the system's eigenvalues were analyzed. The PSS parameter optimization results are shown in Table 4 for each method used in this research, namely, PSO and CRPSO.

Table 3. Voltage Profile

Variation	Step Time	Initial Value	Final Value
Load I	1	0	+0.1
Load II	25	0	+0.1

Table 4. Optimization Results

PSO			CRPSO		
Parameter		Value	Parameter		Value
PID	Kp	0.1370	PID	Kp	11.1975
	Ki	1.3197		Ki	1.6147
	Kd	0.0026		Kd	0.0053
PSS	Kpss	15.3452	PSS	Kpss	48.5261
	T1	0.0161		T1	0.0291
	T2	0.0405		T2	0.0447
	T3	0.3562		T3	0.6169
	T4	0.1096		T4	0.3086

Table 5. Bakaru Generator Speed Overshoot

No PSS	PID-PSS PSO	PID-PSS CRPSO
Load Variation I		
-0.01994 & 0.004966	-0.01418 & 0.0009073	-0.0103 & 0.0002279
Load Variation II		
-0.00142237 & 0.0009883	-0.00105159 & 0.000314361	-0.000628763 & 5.81025e-05

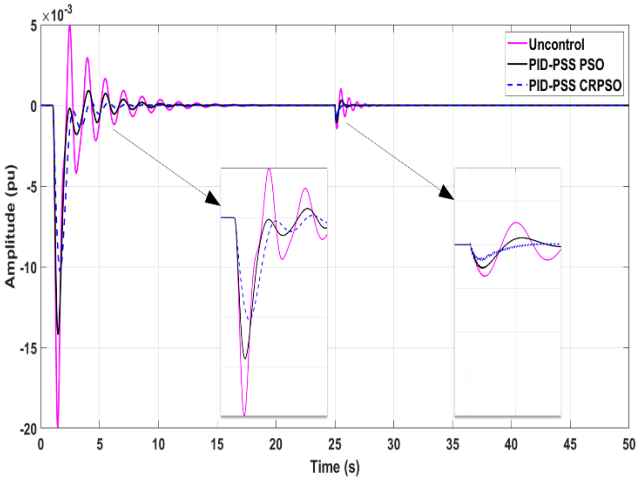

Figure. 12 Speed Response (Δω) of Bakaru

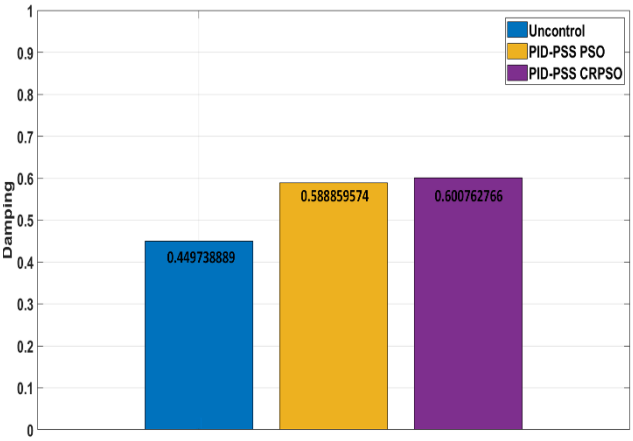

Figure. 13 Damping System

Table 6. Critical Eigenvalue

No PSS (pu) 1.0e+02	PID-PSS-PSO (pu) 1.0e+02	PID-PSS-CRPSO (pu) 1.0e+02
-0.5094 + 6.5474i	-0.5099 + 6.5516i	-0.5094 + 6.5598i
-0.5094 - 6.5474i	-0.5099 - 6.5516i	-0.5094 - 6.5598i
-0.4436 + 5.3193i	-0.4447 + 5.3208i	-0.4447 + 5.3175i
-0.4436 - 5.3193i	-0.4447 - 5.3208i	-0.4447 - 5.3175i
-0.4145 + 5.0618i	-0.4150 + 5.0626i	-0.4133 + 5.0594i
-0.4145 - 5.0618i	-0.4150 - 5.0626i	-0.4133 - 5.0594i
-0.3056 + 4.6944i	-0.3057 + 4.6946i	-0.3058 + 4.6950i
-0.3056 - 4.6944i	-0.3057 - 4.6946i	-0.3058 - 4.6950i
-0.3123 + 4.5315i	-0.3208 + 4.5315i	-0.3260 + 4.5271i
-0.3123 - 4.5315i	-0.3208 - 4.5315i	-0.3260 - 4.5271i
-0.1971 + 4.4656i	-0.0675 + 4.1445i	-0.1943 + 4.4574i
-0.1971 - 4.4656i	-0.0675 - 4.1445i	-0.1943 - 4.4574i
-0.1228 + 4.3282i	-0.1964 + 4.4644i	-0.1377 + 4.2792i
-0.1228 - 4.3282i	-0.1964 - 4.4644i	-0.1377 - 4.2792i
-0.0845 + 4.1601i	-0.1266 + 4.3091i	-0.1970 + 4.3145i
-0.0845 - 4.1601i	-0.1266 - 4.3091i	-0.1970 - 4.3145i
-0.1965 + 4.3135i	-0.1969 + 4.3144i	-0.0138 + 4.0821i
-0.1965 - 4.3135i	-0.1969 - 4.3144i	-0.0138 - 4.0821i
-0.0412 + 3.9001i	-0.2601 + 4.1909i	-0.2692 + 4.2004i
-0.0412 - 3.9001i	-0.2601 - 4.1909i	-0.2692 - 4.2004i
-0.2594 + 4.1886i	-0.0413 + 3.9001i	-0.0413 + 3.9001i
-0.2594 - 4.1886i	-0.0413 - 3.9001i	-0.0413 - 3.9001i
-0.0825 + 4.0439i	-0.0826 + 4.0443i	-0.0830 + 4.0460i
-0.0825 - 4.0439i	-0.0826 - 4.0443i	-0.0830 - 4.0460i
-0.0389 + 3.5546i	-0.0391 + 3.5545i	-0.0395 + 3.5531i
-0.0389 - 3.5546i	-0.0391 - 3.5545i	-0.0395 - 3.5531i
-0.1003 + 2.3007i	-0.0951 + 2.2953i	-0.0622 + 2.2936i
-0.1003 - 2.3007i	-0.0951 - 2.2953i	-0.0622 - 2.2936i
1.7356 + 0.0000i	1.7343 + 0.0000i	1.7272 + 0.0000i
-0.1487 + 1.5167i	-0.1437 + 1.5147i	-0.1446 + 1.5125i
-0.1487 - 1.5167i	-0.1437 - 1.5147i	-0.1446 - 1.5125i
-0.1171 + 1.3752i	-0.1168 + 1.3748i	-0.1154 + 1.3729i
-0.1171 - 1.3752i	-0.1168 - 1.3748i	-0.1154 - 1.3729i
-0.0033 + 0.0410i	-0.0041 + 0.0412i	-0.0062 + 0.0666i
-0.0033 - 0.0410i	-0.0041 - 0.0412i	-0.0062 - 0.0666i
-0.0045 + 0.0462i		
-0.0045 - 0.0462i		

Excitation Voltage Response

To observe the output response, one can analyze the output voltage provided by the PSS by observing the generator's Field Voltage *(E_{fd})*. Installing PID-PSS control on the Bakaru generator provides an additional excitation signal, which is evident in the generator excitation E_{fd} response when load changes occur. Fig. 10 illustrates the generator excitation voltage output characteristics of each control scheme. The analysis results indicate optimal signal performance using PID-PSS-CRPSO, in comparison with other control schemes.

Generator Speed Response

Fig. 11 illustrates the speed response of the Bakaru generator. During the occurrence of both the first and second load changes, the PSS aids in dampening the rotor rotation when the generator's speed decreases. The speed response, including overshoot and settling time values, is detailed in Table 5.

Table 5 displays the speed response characteristics of the Bakaru generator under various load change conditions. Analysis of the first set of load change conditions reveals that the PID-PSS with optimization based on CRPSO exhibits the most optimal performance, with the minimum overshoot response recorded as -0.0103 and 0.0002279pu. Conversely, the system without control demonstrates the poorest response, with values of -0.01994 and 0.004966pu, while PID-PSS-PSO records -0.01418 and 0.0009073pu. In the second set of load change

Table 7. Local Eigenvalue

No PSS (pu) 1.0e+02	PID-PSS-PSO (pu) 1.0e+02	PID-PSS-CRPSO (pu) 1.0e+02
-1.0033 + 9.4208i	-18.4435 + 5.4981i	-18.1450 + 8.2885i
-1.0046 + 8.4406i	-1.4348 + 9.6810i	-1.5534 + 9.5340i
-1.0502 + 7.0767i	-2.7679 + 6.9541i	-2.7561 + 7.3062i
-0.8534 + 7.0320i	-1.1885 + 7.1622i	-0.6229 + 6.6623i
-1.4621 + 6.0622i	-0.8479 + 6.9048i	-2.2016 + 5.3794i
-0.7893 + 5.3314i	-1.5843 + 5.6341i	-1.4080 + 5.9675i
-1.2483 + 5.8288i	-1.1383 + 5.7984i	-1.0180 + 5.5285i
-0.9420 + 5.4922i	-0.8488 + 5.3313i	-0.9279 + 5.3410i
-1.1605 + 5.7451i	-1.3109 + 5.5865i	-1.4050 + 5.5193i
-1.1515 + 5.6619i	-0.9475 + 5.4760i	-1.6177 + 5.2963i
-1.1481 + 5.6585i	-1.2159 + 5.6935i	-1.4176 + 5.4353i
-0.9914 + 5.4659i	-0.9945 + 5.4675i	-1.0036 + 5.4648i

Table 8. Inter-Area Eigenvalue

No PSS (pu) 1.0e+02	PID-PSS-PSO (pu) 1.0e+02	PID-PSS-CRPSO (pu) 1.0e+02
-0.3324 + 4.0969i	-48.6564 + 3.0524i	-6.3303 + 2.5647i
-0.4455 + 4.6250i	-8.5759 + 1.3271i	-0.5839 + 4.5908i
-0.5006 + 4.5944i	-0.4099 + 4.1229i	-2.7646 + 4.7640i
-0.5131 + 4.5342i	-1.7558 + 4.6381i	-3.2821 + 2.3975i
	-0.5110 + 4.6153i	-0.5799 + 4.0755i
	-2.0859 + 4.7848i	
	-1.7253 + 1.9749i	

conditions, the PID-PSS system demonstrates a minimal overshoot response of -0.000628763 and 5.81025e-05pu, while the largest overshoot occurs in the scheme without control, with values of -0.00142237 and 0.000988391pu. The PID-PSS-PSO system registers an overshoot of -0.00105159 and 0.000314361pu.

Generator Rotor Angle Response

Fig. 12 displays the rotor angle response of the Bakaru generator under various control schemes. The PID-PSS-CRPSO-based control scheme demonstrates optimal performance, characterized by minimal overshoot during both the first and second load changes. Furthermore, its fast settling time enables the generator to return to steady-state operating conditions swiftly.

Damping System

Fig. 13 presents the total system damping under various control schemes. The proposed control scheme based on PID-PSS-CRPSO achieves a maximum damping value of 0.600762766. In contrast, the system without PSS exhibits the minimum damping value of 0.449738889, while the system with PID-PSS-PSO achieves a damping value of 0.588859574.

PID-PSS, or Proportional-Integral-Derivative Power System Stabilizer, is a component that generates control signals directed to the excitation system. Its primary function is to enhance stability by regulating the excitation performance of the synchronous generator rotor. The excitation system of a generator supplies direct current (DC) to reinforce the electric generator or serve as a magnetic field generator. This ensures that the generator can produce electrical energy with a high output voltage, dependent on the magnitude of the excitation current.

Eigenvalue Analysis

This section presents the eigenvalue performance analysis of systems without PSS, with PID-PSS-PSO, and with PID-PSS-CRPSO. The analysis includes critical eigenvalues (Table 6), local eigenvalues (Table 7), and inter-area eigenvalues (Table 8). These tables depict the behavior of the system eigenvalues under each control scheme studied. In general, the tables demonstrate an increase in the system's eigenvalues with the application of various control schemes. This increase is evident from the eigenvalues' shift towards the left, accompanied by a more negative real part (σ). A more negative real part signifies enhanced system stability. Particularly, PID-PSS-CRPSO exhibits effectiveness in

augmenting the eigenvalue and damping of the system. Improved eigenvalues contribute to overall system stability and performance.

5. Conclusion

The performance of the Sulselrabar system reaches optimization when the SVC and PID-PSS are installed and properly tuned. This study presents an optimization approach for SVC and PID-PSS based on CRPSO, known for its effectiveness in optimization problems. The computational process using CRPSO surpasses conventional PSO, as evidenced by the PSO-based fitness function value of 9.39E+07 converging in the 21st iteration, whereas CRPSO achieves convergence faster, attaining a value of 9.38E+07 in the 11th iteration. The optimal location for SVC installation is identified as Bus 31, with optimal parameter tuning of 40 MVar for PSO and 80 MVar for CRPSO. Implementing CRPSO-based SVC installation and tuning results in optimal power flow in the South Sulawesi system, leading to an improved voltage profile and minimized line losses. Furthermore, system stability during N-1 contingency conditions is upheld through optimal implementation of PID-PSS. The system's damping is maximized by employing a CRPSO-based PID-PSS control scheme, yielding a damping factor of 0.600762766 compared to other control schemes. Increased stability is also obtained from the system's increasingly negative eigenvalues.

Notation List

Parameters	Notation
B_{svc}	Susceptance
V	Bus voltage
Q_{svc}	Reactive power injected by an SVC
K_A	SVC Gain
T_A	Time constant
V_{Rmin}, V_{Rmax}	The max and min output of exciter
V_s	The output of the PSS
K_{PSS}	The PSS gain
T_w	The washout filter
T_1, T_2, T_3, T_4	The lead-lag gains
f	The oscillation frequency
λ_i	The eigenvalue
σ_i	The real component of the eigenvalue
ω_i	The eigenvalue imaginary component
CDI	Comprehensive damping index
ζ_i	Damping ratio
ζ_{min}	Minimum damping
P_{best}	Own best experience Particle
G_{best}	The collective best experience Particle
x^k	Current search point
x^{k+1}	The modified search position
v^k	The current speed
v^{k+1}	The modified speed
V_{pbest}	The speed based on p_{best}
V_{gBest}	Denotes the speed based on G_{best}
m	r number of members in the particle
p_{best-i}	P_{best} from the current iteration
g_{best-i}	G_{best} from the group
w	Stands for the weight
c_i	The weight coefficient
c_1, c_2	Two positive constants
r_1, r_2	Random numbers ranging from 0 to 1

Conflicts of Interest

The authors declare no conflict of interest.

Author Contributions

Conceptualization, Makmur Saini, Muhammad Ruswandi Djalal; methodology, Makmur Saini and Muhammad Ruswandi Djalal; software, Muhammad Ruswandi Djalal; Validation, Makmur Saini and Muhammad Ruswandi Djalal; formal analysis, Muhammad Ruswandi Djalal and A.M. Shiddiq Yunus; investigation, Makmur Saini and Muhammad Ruswandi Djalal; resources, Muhammad Ruswandi Djalal; writing original draft preparation, Muhammad Ruswandi Djalal; writing review and editing, A.M. Shiddiq Yunus; visualization, Muhammad Ruswandi Djalal, All authors have read and agreed to the published version of the manuscript.

Acknowledgments

The author expresses gratitude to the Ministry of Education, Culture, Research, and Technology (Kemendikbudristek) and P3M Ujung Pandang State Polytechnic for their support in conducting this research.

References

[1] J. K. P. Desai and V. Makwana, *Power Swing Detection and Generator Out-of-Step Protection Under Renewable Power Source Integration*, Springer Nature, 2023.

[2] N. Hatziargyriou et al., "Definition and classification of power system stability–revisited & extended", *IEEE Transactions on Power Systems*, Vol. 36, No. 4, pp. 3271-3281, 2020, doi: 10.1109/TPWRS.2020.3041774.

[3] V. Vittal, J. D. McCalley, P. M. Anderson, and A. Fouad, *Power System Control and Stability*. John Wiley & Sons, 2019.

[4] J. Shair, H. Li, J. Hu, and X. Xie, "Power system stability issues, classifications and research prospects in the context of high-penetration of renewables and power electronics", *Renewable*

and Sustainable Energy Reviews, Vol. 145, p. 111111, 2021, doi: 10.1016/j.rser.2021.111111.

[5] H. M. Alasooly, *Control of Flexible Alternating Current Transmission System (FACTS) for Power Stability Enhancement*, BookRix, 2020.

[6] F. Z. Peng, "Flexible AC transmission systems (FACTS) and resilient AC distribution systems (RACDS) in smart grid", In: *Proc. of the IEEE*, Vol. 105, No. 11, pp. 2099-2115, 2017, doi: 10.1109/JPROC.2017.2714022.

[7] B. Bhattacharyya and V. K. Gupta, "Fuzzy based evolutionary algorithm for reactive power optimization with FACTS devices", *International Journal of Electrical Power & Energy Systems*, Vol. 61, pp. 39-47, 2014, doi: 10.1016/j.ijepes.2014.03.008.

[8] S. Dutta, P. K. Roy, and D. Nandi, "Optimal location of UPFC controller in transmission network using hybrid chemical reaction optimization algorithm", *International Journal of Electrical Power & Energy Systems*, Vol. 64, pp. 194-211, 2015, doi: 10.1016/j.ijepes.2014.07.038.

[9] E. Naderi, M. Pourakbari-Kasmaei, and H. Abdi, "An efficient particle swarm optimization algorithm to solve optimal power flow problem integrated with FACTS devices", *Applied Soft Computing*, Vol. 80, pp. 243-262, 2019, doi: 10.1016/j.asoc.2019.04.012.

[10] A. Mukherjee and V. Mukherjee, "Solution of optimal power flow with FACTS devices using a novel oppositional krill herd algorithm", *International Journal of Electrical Power & Energy Systems*, Vol. 78, pp. 700-714, 2016, doi: 10.1016/j.ijepes.2015.12.001.

[11] D. Prasad and V. Mukherjee, "A novel symbiotic organisms search algorithm for optimal power flow of power system with FACTS devices", *Engineering Science and Technology, an International Journal*, Vol. 19, No. 1, pp. 79-89, 2016, doi: 10.1016/j.jestch.2015.06.005.

[12] P. P. Biswas, P. Arora, R. Mallipeddi, P. N. Suganthan, and B. K. Panigrahi, "Optimal placement and sizing of FACTS devices for optimal power flow in a wind power integrated electrical network", *Neural Computing and Applications*, Vol. 33, No. 12, pp. 6753-6774, 2021, doi: 10.1007/s00521-020-05453-x.

[13] B. Mahdad, K. Srairi, and T. Bouktir, "Optimal power flow for large-scale power system with shunt FACTS using efficient parallel GA", *International Journal of Electrical Power & Energy Systems*, Vol. 32, No. 5, pp. 507-517, 2010, doi: 10.1016/j.ijepes.2009.09.013.

[14] H. Sita, P. U. Reddy, and R. Kiranmayi, "Optimal location and sizing of UPFC for optimal power flow in a deregulated power system using a hybrid algorithm", *International Journal of Ambient Energy*, Vol. 43, No. 1, pp. 1413-1419, 2022, doi: 10.1080/01430750.2019.1707116.

[15] J. Aghaei, M. Gitizadeh, and M. Kaji, "Placement and operation strategy of FACTS devices using optimal continuous power flow", *Scientia Iranica*, Vol. 19, No. 6, pp. 1683-1690, 2012, doi: 10.1016/j.scient.2012.04.021.

[16] H. Ambriz-Pérez, E. Acha, and C. R. Fuerte-Esquivel, "TCSC-firing angle model for optimal power flow solutions using Newton's method", *International Journal of Electrical Power & Energy Systems*, Vol. 28, No. 2, pp. 77-85, 2006, doi: 10.1016/j.ijepes.2005.10.003.

[17] A. H. Halim, I. Ismail, and S. Das, "Performance assessment of the metaheuristic optimization algorithms: an exhaustive review," *Artificial Intelligence Review*, Vol. 54, No. 3, pp. 2323-2409, 2021, doi: 10.1007/s10462-020-09906-6.

[18] M. Saini, M. R. Djalal, A. S. Yunus, and A. Pangkung, "FACTS Devices Optimization for Optimal Power Flow Using Particle Swarm Optimization In Sulselrabar System", *Przeglad Elektrotechniczny*, Vol. 4, 2024, doi: 10.15199/48.2024.04.13.

[19] N. A. Firdausanti, "On the comparison of crazy particle swarm optimization and advanced binary ant colony optimization for feature selection on high-dimensional data", *Procedia Computer Science*, Vol. 161, pp. 638-646, 2019, doi: 10.1016/j.procs.2019.11.167.

[20] M. Ali, M. R. Djalal, H. Nurohmah, and Rukslin, "Intelligent Optimization Using Craziness Particle Swarm on Permanent Magnet Synchronous Motor", In: *Proc. of 2022 2nd International Seminar on Machine Learning, Optimization, and Data Science (ISMODE)*, pp. 579-583, 2022, doi: 10.1109/ISMODE56940.2022.10180931.

[21] S. K. Saha, R. Kar, D. Mandal, and S. P. Ghoshal, "An Efficient Craziness Based Particle Swarm Optimization Technique for Optimal IIR Filter Design", In: *Proc. of Transactions on Computational Science XXI: Special Issue on Innovations in Nature-Inspired Computing and Applications*, pp. 230-252, 2013.

[22] J. Shea, "Understanding FACTS-concepts and technology of flexible AC transmission systems [Book Review]", *IEEE Electrical Insulation Magazine*, Vol. 18, No. 1, pp. 46-46, 2002, doi: 10.1109/MEI.2002.981326.

[23] V. Ajjarapu and C. Christy, "The continuation power flow: a tool for steady state voltage stability analysis", *IEEE Transactions on Power Systems*, Vol. 7, No. 1, pp. 416-423, 1992, doi: 10.1109/59.141737.

[24] I. Robandi, M. R. Djalal, and M. A. Prakasa, "Performance Improvement of Sulselrabar System Using Single-Band Power System Stabilizer Based on Mayfly Algorithm Under Different Loading Condition", *International Journal of Intelligent Engineering & Systems*, Vol. 17, No. 1, pp. 370-382, 2024, doi: 10.22266/ijies2024.0229.33.

[25] M. Mansur and M. R. Djalal, "Using Particle Swarm Optimization for Power System Stabilizer and energy storage in the SMIB system under load shedding conditions", *SINERGI*, Vol. 27, No. 8, pp. 423-432, 2023, doi: 10.22441/sinergi.2023.3.013.

[26] A.-A. A. Mohamed, Y. S. Mohamed, A. A. M. El-Gaafary, and A. M. Hemeida, "Optimal power flow using moth swarm algorithm", *Electric Power Systems Research*, Vol. 142, pp. 190-206, 2017, doi: 10.1016/j.epsr.2016.09.025.

[27] K. M. Metweely, G. A. Morsy, and R. A. Amer, "Optimization of optimal power flow problems with FACTS devices using PSO technique", In: *Proc. of 2017 Nineteenth International Middle East Power Systems Conference (MEPCON)*, 2017, pp. 181-189, doi: 10.1109/MEPCON.2017.8301182.